Anal. Bioanal. Electrochem., Vol. 5, No. 2, 2013, 236 -254

Analytical & Bioanalytical Electrochemistry

Full Paper

Opuntia Ficus Indica Seed Oil:Characterization and Application in Corrosion Inhibition of Carbon Steel in Acid Medium

Hind Hammouch[1,*], Ahmed Dermaj[1], Driss Chebabe[1], Pascal Decaro[2], Najat Hajjaji[1], Naima Bettach[1], Hisasi Takenouti [3] and Abdellah Srhiri [4]

[1]*Laboratoire d'Electrochimie de Corrosion et d'Environnement, Faculté des Sciences, Kenitra, Morocco*

[2]*Laboratoire de Chimie Agro-Industrielle,ENSIACET, 4 alleé Emile Monso-BP 44362, 31030 Toulouse Cedex 4*

[3]*Laboratoire Interfaces et Systèmes Electrochimiques, CNRS-UPR15, UPMC, Paris, France*

[4]*Servichim, 101 Rue Maamoura, N° 10 Kenitra, Morocco*

*Corresponding Author, Tel.:+2125 37 32 94 14; Fax: +212 5 37 32 94 33

E-Mail: hamhind@yahoo.fr

Received: 28 January 2013 / Received in revised form: 9 April 2013/
Accepted: 13 April 2013 / Published online: 30 April 2013

Abstract- The aim of this work is to characterise seed oil of *opuntia ficus indica* and to develop a new formulation to inhibit carbon steel corrosion in acidic medium. "OTH", is a new environmentally friendly corrosion inhibitor containing *Opuntia ficus indica* seed oil. Fatty acid composition was analysed by Gas-chromatography after transesterification to Fatty Methyl esters (FAMES). The Electrochemical Impedance Spectroscopy (EIS) and voltamperometry measurements were carried out for different concentrations and immersion times. Surface analyses were carried out by Scanning Electron Microscopy (SEM) and Energy Dispersive X-ray Spectroscopy (EDS). The results obtained show that the main fatty acids of prickly pear seed oil were C16:0, C18:0, C18:1, C18:2. The content of unsaturated fatty acids was high (83%). Electrochemical measurements show that OTH acts as a good mixed corrosion inhibitor. This inhibitor formulation forms a thick film that plays a barrier layer on the iron surface to minimize the contact area with corrosive solution and hinder metal oxidation.

Keywords- Opuntia Ficus Indica, Corrosion Inhibition, Carbon Steel, EIS

1. INTRODUCTION

Opuntia ficus indica (nopal or prickly pear cactus), is much known in Morocco for its edible fruits, and its stems used as animal's food. Also *Opuntia* has an important ecological role in combating erosion, and it is adapted in the agricultural production system of arid and semi–arid regions. The cactus fruits have a high anti-oxidant activity due to the presence of vitamin C, polyphenols and betalains pigments. The seeds are rich in oil, known for its content in polyunsaturated fatty acids [1-4].

Iron is the most commonly used metallic material in all industrial process, due to its low cost. Unfortunately it is a subject of corrosion phenomena that become important particularly in acidic media. This is the reason that a development of protection systems is an important issue. The use of corrosion inhibitors is one of the most cost effective methods. Therefore a development of safe corrosion inhibitors called "environmentally friendly corrosion inhibitors" is required [5]. Indeed, these last years many scientific research are devoted in this topic and several studies concern the development of effective products containing biodegradable and innoxiously vegetal molecules [6-10]. In this study we develop a new corrosion inhibitor based on *Opuntia ficus indica* seed oil noted OTH, to protect carbon steel samples.

The inhibition efficiency was evaluated by means of electrochemical measurements. The surface morphology was observed by SEM which leads to note the presence of inhibitor on carbon steel sample surface.

2. MATERIAL AND METHODS

2.1. Oil Extraction

Mature prickly pear fruits collected in august, were hand-peeled, the pulp was separated from the seeds. These seeds were washed with water and dried at ambient temperature in the shade and then ground to obtain a seed powders.

The oil was extracted with cyclohexane in soxhlet extractor for 7 h. Organic phase was removed using a rotary evaporator; the oil obtained was filtered and stored at 4 °C.

2.1.1. Physicochemical analyses

Refractive index was determined at 20 °C with universal refractometer; density was determined with pyknometer. Saponification index, unsaponifiable matter and acid index were determined.

2.1.2. Fatty acid analysis

Fatty acids were transesterified into methyl esters FAME with 2 M KOH in methanol at 60 °C. FAME were identified on CPG GC3900FAME 2010, CP select CB for FAME fused

silica WCOT (50 m×0.25×0.25 µm film thickness), equipped with flame ionisation detector (FID). The flow rate of the carrier gas helium was 1.2 mL/min. The injector and FID temperatures were set at 250 °C. The initial column temperature was 140 °C programmed by 5 °C /min to 180 °C and kept 5 min at 180 °C, then 45 °C/min until 250 °C and kept 10 minutes at 250 °C.

Identification and quantification of FAMES was accomplished by comparing the retention times of peaks with those of pure standard analysed under the same conditions. The results were expressed as a percentage of individual fatty acids in the lipid fraction.

2. 2. Electrochemical measurements

2.2.1. Solution

The electrolyte used in this study was 0.2 g L^{-1} Na_2SO_4+0.2 g L^{-1} $NaHCO_3$+0.2 g L^{-1} NaCl (pH 3.6). The resistivity of this solution was approximately 1 kΩcm. This solution noted (IRW), may correspond approximately to rainwater in urban area near seaside with high degree of pollution (industrial atmosphere).

2.2.2. Corrosion inhibitor "OTH"

The corrosion inhibitor used noted OTH based on seed oil of *Opuntia ficus indica* .This product was patented in Morocco [11].OTH is essentially based on fatty acid of *Opuntia*, triethanolamine and KOH. This inhibitor was added in the corrosive solution at the concentration of 0.05; 0.1 and 0.2 vol-%.

2.3. Surface analyses

Scanning electron microscopy (SEM) studies were performed with Leica Stereoscan 440 coupled with EDS elemental semi-quantitative analyses (Princeton Gamma-Tech).

2.4. Experimental setup

The samples used in this study were made of carbon steel having a composition shown in Table 1.

Table 1. Composition of carbon steel determined by EDS analysis

Element	**Si**	**Mn**	**C**	**P**	**S**	**Fe**
Wt %	0.201	0.519	0.157	0.007	0.009	≥ 99

Three-electrode cell was used for electrochemical measurements. The volume of electrolyte was ca. 50 mL. The reference electrode was saturated calomel (SCE) and all potentials are referred to this electrode without any correction. The counter electrode was platinum gauze of which surface is much greater than the working electrode.

All electrochemical measurements were carried out with a Gamry potentiostat (model FAS-1).The EIS experiments were performed using a 10 mV_{rms} at the open circuit corrosion potential (E_{corr}) from 100 kHz to 10 mHz with frequency interval of 10 points per decade. These measurements were operated in Faraday cage to minimise ambient electrical noises. The working electrode was rotating disk at 600 rpm (Tacusel-Radiometer, ED1).

3. RESULT AND DISCUSSION

3.1. Oil content

Opuntia ficus indica seed oil content is represented in Table 2, and compared with literature.

Table 2. Oil content for *Opuntia ficus indica* seed oil

Authors	**country of study**	**Oil content**
Boujnah , 2000 [12]	Morocco	9%
Salvo et al., 2002 [13]	Italy	9.14%
Yalçin et al., 2003 [3]	Turkey	6.19%
Ennouri et al., 2005 [4]	Tunisia	10.9%
Tlili et al., 2011 [14]	Tunisia	5.5%
This study 2011	Morocco	9%

The difference observed is probably due to the origin of the fruits, and period of ripening. The climatic conditions and environmental factors such as light, temperature and water stress might affect oil content as reported by literature [15].

3.2. Physicochemical characteristics and Fatty acid profile

The density of the seed oil at 20 °C, the refractive index and saponification index compared favourably with literature Table 3. The differences observed are probably done to the origin of the fruits, climatic conditions and degree of maturity of the fruit.

Oleic and linoleic acids are the major fatty acids found in oil seeds. Fatty acid composition of *Opuntia* oil is summarized in Table 4 and compared with literature. The cactus oil contained high amounts of oleic (18:1,20%) and linoleic (18:2,61%) acids, and low amounts of palmitic (16:0,13%) and stearic (18:0,4%) acids. These results are in agreement with those of El Mannoubi et al. [16]. The observed difference is possibly due to the degree of maturity of the fruit.

Opuntia seed oil contained high amounts of polyunsaturated (linoleic acid), and moderate amounts of monounsaturated oleic acid. Unsaturated total fatty acids are prevalent (83%). This prevalence of the unsaturated fatty acids and the high values of the iodine index indicate that the oil of *opuntia ficus indica* is of *the unsaturated type.*

Table 3. Physicochemical characteristics of *Opuntia ficus indica* seed oil

Constante	**value**	**Literature [1,2,4,13]**
Density at 20 °C	0.8901	0.9-0.9168
Refractive index 20 °C	1.4666	1.459–1.475
saponification index (mg deKOH /g)	141	174-222
unsaponifiable matter%	0.8	1.34-4
Acid index (mg KOH / g)	3.79	0.28
Iodine index (g/100 g)	165	101-131
Peroxide index (meq 0_2 / Kg of oil)	5.5	1.84-10

Table 4. Fatty acid composition of *Opuntia ficus indica* seed oil

Fatty acids		**Amounts of fatty acid (%)**	**Literature [3, 14, 16, 17]**
Palmitic acid	C16 :0	13,52	12.23-13.21
Palmitoleic acid	C16 :1	0,77	0.12-1.85
Stearic acid	C18 :0	4,06	3.31-4 .79
Oleic acid	C18 :1	19,81	20.19-25.6
Linoleic acid	C18 :2	61,14	52.25-61.01
Arachidic acid	C20:0	0.7	0.36-0.66

3.3. Electrochemical results

3.3.1. Surface analyses

SEM observations were carried out after 24 h of immersion of carbon steel in presence and in absence of 0.2% of inhibitor (Fig. 1).

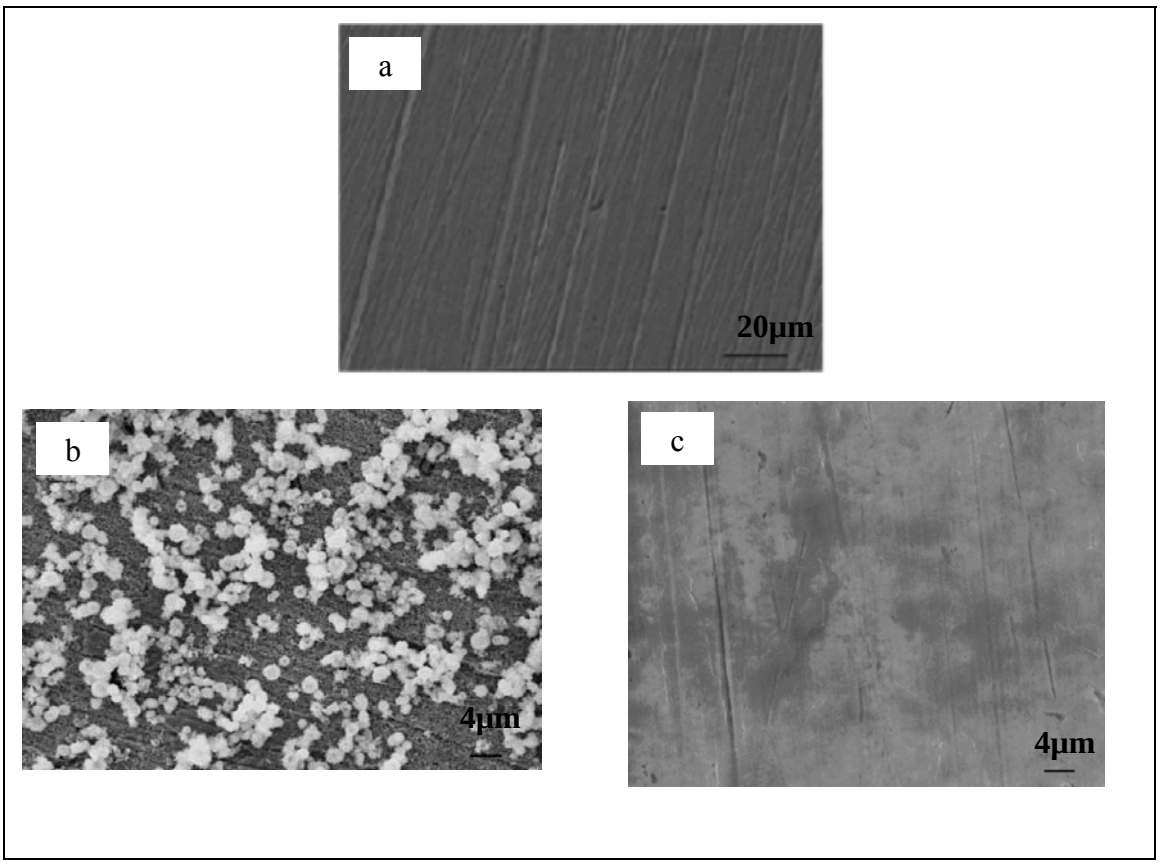

Fig. 1. SEM pictures (backscattered electrons) of carbon steel in presence and absence of 0.2% of inhibitor after 24 h of immersion rotated rat 600 rpm (a) Carbon steel surface before experiment,(b) Carbon steel surface in (IRW) without inhibitor during 24 h, (c) Carbon steel surface in (IRW) with 0.2% of OTH during 24 h

In absence of OTH, the metallic surface is heavily corroded as can be seen in Fig. 1-b, the SEM picture presents morphologies "cotton balls" and "rosette" typical of akaganeite (*β-FeOOH)* a component of rust developed in marine atmospheres [18].

When OTH was added into the corrosion test solution (IRW), a smooth surface was noticed traducing a good protection effect of the corrosion inhibitor by a formation of a thick and compact film.

The results of EDS analyses are represented in Fig. 2. In the blank test solution, a marked peak of O is observed indicating that in this slightly acidic medium, the iron oxide was formed and covering the electrode surface. In presence of 0.2% of OTH, the presence of carbon can be seen clearly whereas the peaks relative to Fe decreased significantly; the formation of thick inhibitor layer can be ascertained.

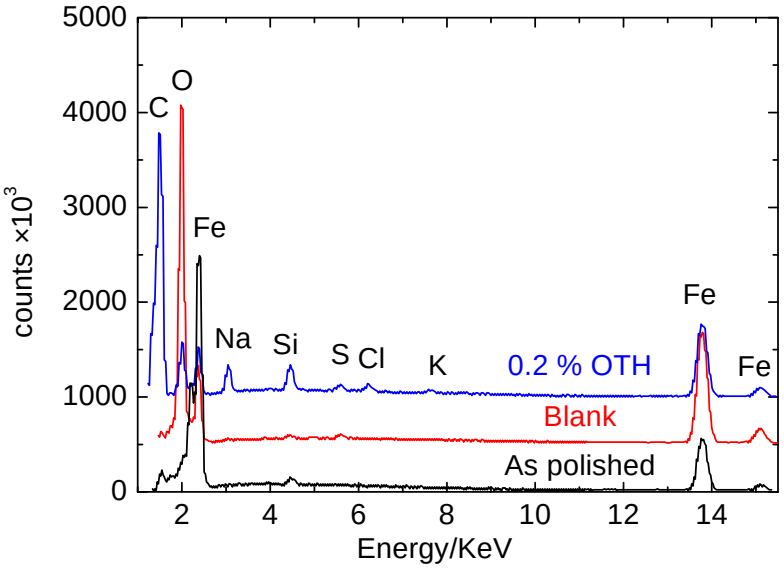

Fig. 2. EDS spectra for the electrode surface of carbon steel corresponding to the surface of SEM picture presented in Fig. 1: (a) as polished, (b) Blank, and (c) in presence of 0.2% OTH

3.3.2. Voltamperometric experiments

The cathodic and anodic polarization curves were collected after two h of immersion at the open circuit conditions in IRW at various concentrations of OTH.

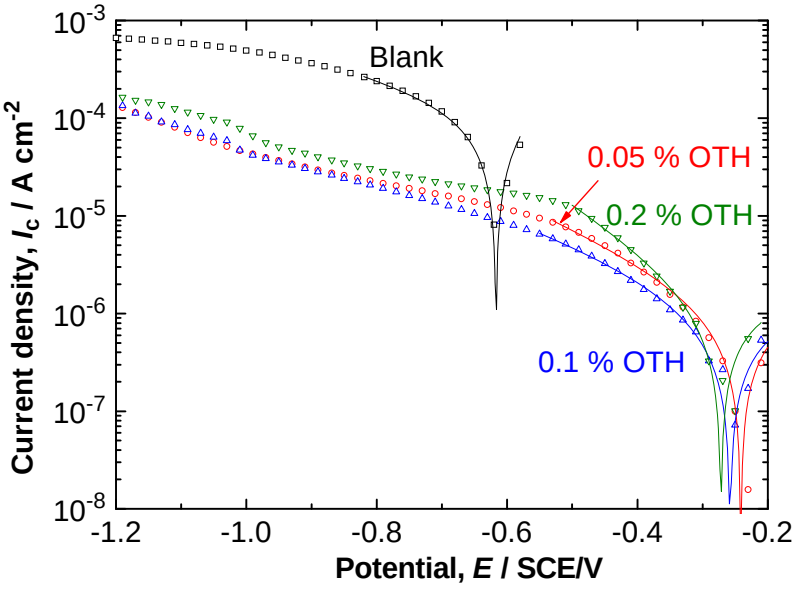

Fig. 3. Cathodic polarization curves of carbon steel in IRW with various OTH concentrations. Rotating disk electrode at 600 rpm

3.3.2.1. Cathodic polarization

After two h of stabilization period, the current–potential relationship was collected by potential dynamic method, at 10 mV s^{-1}. The potential scan started from 10 mV more positive than the open circuit one (E_{corr}), and finished at 0.5 V more negative than E_{corr}. as shown in Fig. 3.

On this figure, it can be seen that the addition of corrosion inhibitor into the IRW solution induces a marked decrease of cathodic current density values for the OTH concentration as low as 0.05% of OTH. The corrosion potential E_{corr} is low as –0.617 V/ SCE in absence of inhibitor indicating the corrosion at an active state. In contrast, in presence of 0.2% OTH E_{corr} becomes around -0.272 V/SCE. This potential corresponds well to the corrosion of iron in the passive state. This marked shift of corrosion potential may indicate an important anodic inhibiting effect of OTH even though the cathodic current densities also decreased significantly.

Around the open circuit corrosion potential, it is considered that the current observed can be expressed by so called the Stern-Geary relationship [19]:

$$I = I_{corr} \{\exp[b_a \cdot (E-E_{corr})] - \exp[b_c \cdot (E-E_{corr})]\} \quad (1)$$

Where b_a and b_c are the anodic and cathodic Tafel constants (reciprocal of Tafel slope in neparian scale) respectively. A non-linear regression calculation was applied to evaluate these kinetical parameters. The potential domain used in this calculation is limited from the starting potential to 0.2 or 0.3 V/SCE more negative than E_{corr}. If wider potential range was selected, then a significant divergence was observed between experimental and calculated data indicating that Eq. (1) is no longer valid. The results of calculation are reported in Table 5.

Table 5. Kinetic parameters determined from the cathodic potential scan. Carbon steel in IRW. Electrode rotation speed at 600 rpm

OTH (%)	E_{corr} (SCE/V)	I_{cor} (µA cm^{-2})	*b*a (V^{-1})	b_c (V^{-1})	I.E. (%)
0	-0.617	107	9.92	-4.75	-
0.05	-0.241	1.27	2.4	-6.99	98.8
0.1	-0.258	1.57	0.96	-5.49	98.5
0.2	-0.272	1.37	1.88	-10.1	98.7

On this table, the inhibiting efficiency (I.E.) was calculated according to the equation below.

$$I.E. = 100 \cdot \frac{I_{corr,0} - I_{corr}}{I_{corr,0}} \quad (2)$$

The inhibiting efficiency is greater than 98.5% indicating an excellent protective effect of OTH.

3.3.2.2. Anodic polarization

Anodic polarization curves were obtained, as in the cathodic curves case, after two h of immersion time at the open circuit conditions. In this plot, the potential scan was started at 10 mV more negative than E_{corr} and ended at 1 V/SCE. Fig. 3 presents the obtained results.

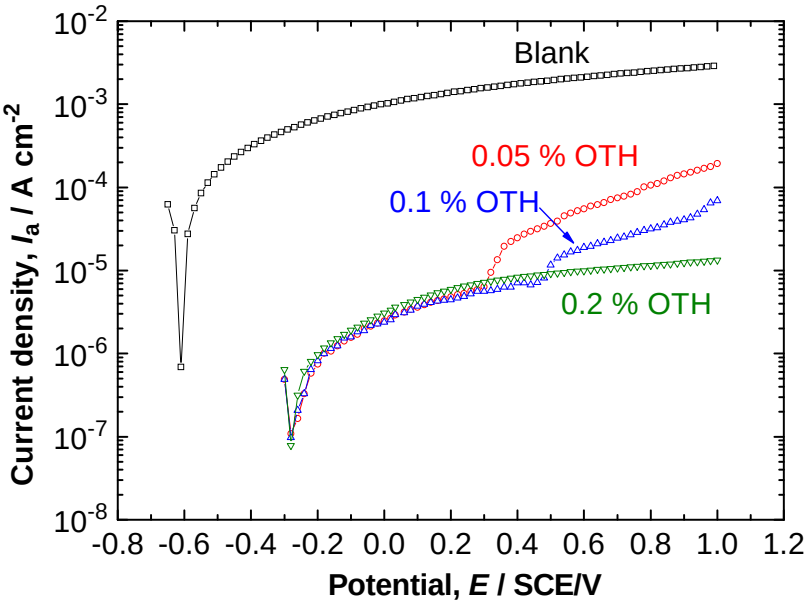

Fig. 3. Anodic polarization curves of carbon steel in IRW in presence of various OTH concentrations. Disk rotation speed at 600 rpm

In absence of OTH, anodic current density value increases smoothly with anodic potential increase. This variation characterizes that charge transfer process taking place at the electrode surface. A linear increase of current in this semi-logarithmic scale corresponds to an electrochemical system governs by charge transfer process through activation energy. It is important to note that, even in the potential domain corresponding to the passive state, the anodic current remains high, and no passivation process is observed. This behaviour can be associated with the presence of significant amount of chloride ions in IRW.

In presence of inhibitor, the current density values decrease dramatically, for instance more than 400 times at 0 V/SCE compared to obtained value without inhibitor. This low current density in presence of OTH corroborates an iron surface in the passive state. However, a steep increase of the anodic current density was observed at about 0.30 and 0.49

V/SCE respectively in presence of 0.05 and 0.1% OTH. No such current increase was observed in the potential domain examined when 0.2% of OTH was added into IRW. The current increase observed will be associated with the pitting initiation beneath the inhibitor film. However, the presence of this film hinders efficiently the propagation of pitting, thus the current density remains relatively low. The kinetic parameters of corroding electrode on the basis of the Stern–Geary expression were determined by a non-linear regression calculation. Fig. 4, presents the comparison between experimental and calculated data.

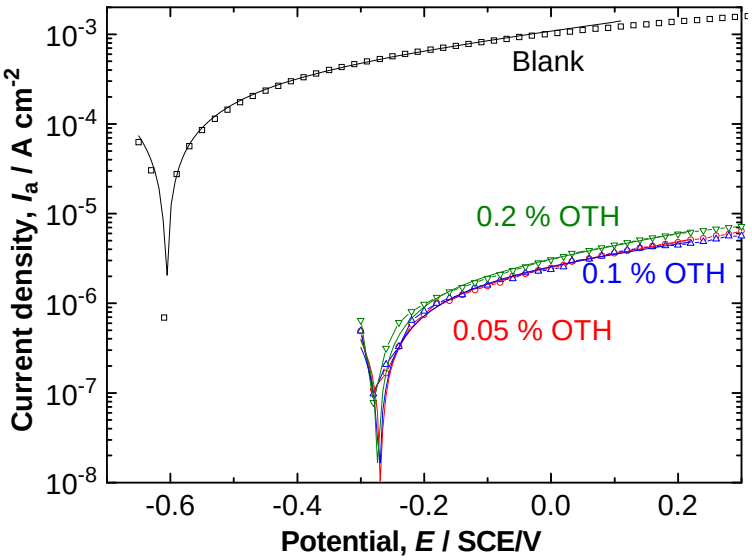

Fig. 4. Anodic current densities evaluated by Stern-Geary relationship in absence and in presence of OTH. Disk rotation speed at 600 rpm

The results of regression calculation are summarized in Table 6.

Table 6. Kinetic parameters determined from the anodic potential scan. Carbon steel in IRW. Disk rotation speed at 600 rpm

OTH (%)	E_{corr} (SCE/V)	I_{corr} (μA cm^{-2})	b_a (V^{-1})	b_c (V^{-1})	I.E. (%)
0	-0.607	294	2.21	-3.4	
0.05	-0.269	1.30	2.85	-5.99	99.6
0.1	-0.271	1.80	2.12	-3.88	99.4
0.2	-0.273	1.54	2.92	-6.13	99.5

The values of corrosion current density determined in presence of OTH by the cathodic and the anodic potential scan are similar. In contrast, in absence of inhibitor, I_{corr} is three times greater than that of anodic potential scan. The origin of this discrepancy is unknown, but the corrosion current density is often less reproducible variable. From this table, one can

conclude, as the case of cathodic scan, the addition of OTH as low as 0.05% gives an excellent inhibitive effect.

3.4. Electrochemical impedance spectroscopy (EIS)

3.4.1. Influence of OTH concentration

Fig. 5 shows the EIS spectra in Nyquist plots of carbon steel. The impedance spectra was started after 2 h of immersion in IRW at the rest potential with and without OTH to avoid too fast change of open circuit corrosion potential.

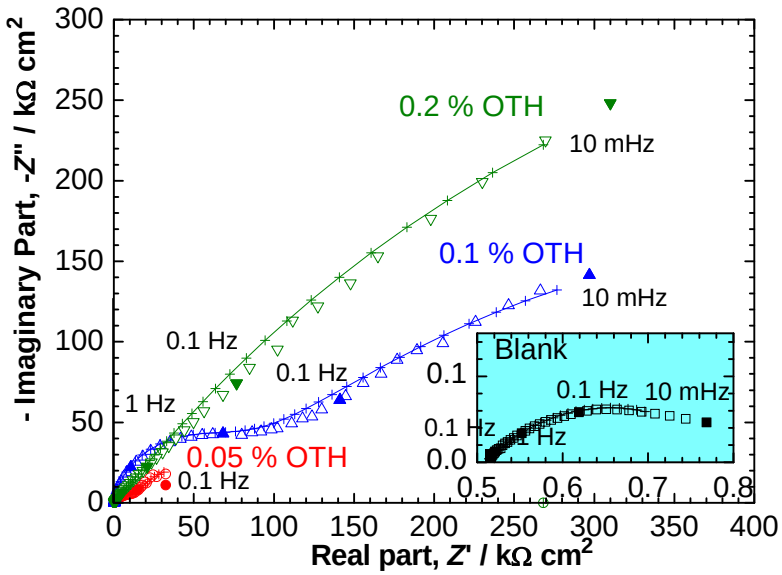

Fig. 5. EIS spectra of carbon steel in IRW, after 2 h of immersion. Disk rotation speed=600 rpm. Some frequencies at which the impedance was measured are also indicated together with OTH concentration

In the absence of OTH, the Nyquist diagrams indicated in the insert present one depressed semicircle. In presence of OTH, two capacitive loops were observed, clearly seen in 0.05 and 0.1% OTH. The two loops were overlapped, and become hardly to be distinguished at higher inhibitor concentration. According to this observation, the following electrical equivalent circuit was proposed Fig. 6.

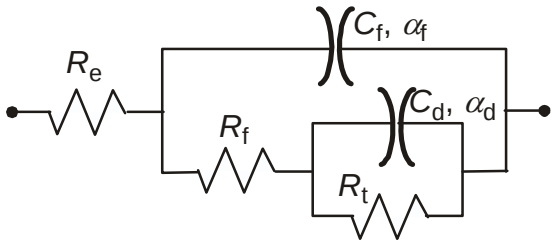

Fig. 6. Electric equivalent circuit

The origin of the circuit elements are as follows:

R_e : Electrolyte resistance (Ω cm^2)

R_f : Film resistance due to the ionic conduction through inhibitor layer (Ω cm^2)

C_f : Film capacitance due to the electronic insulating property (F cm^{-2})

R_t : charge transfer resistance (Ω cm^2)

C_d : Double layer capacitance at the metal electrolyte interface (F cm^{-2})

α_f, α_d: Cole-Cole coefficient representing a depressed shape in Nyquist diagram.

The impedance of Cole-Cole type behaviour is expressed by the equation below:

$$Z = \frac{R}{1 + (\mathrm{j} \cdot \omega \cdot R \cdot C)^{\alpha}} \tag{3}$$

This equation contrasts to CPE (Constant Phase Element) impedance, often used in these days:

$$Z = \frac{1}{\frac{1}{R} + Q \cdot (\mathrm{j} \cdot \omega)^{\alpha}} \tag{4}$$

The results of regression calculation of these impedance data by lab-made simplex software are overlaid on the Nyquist plot presented in Fig. 5. Except for the results obtained in presence of 0.2% OTH, agreement between experimental and calculated data is satisfactory. Some systematic errors were observed, in contrast for the latter, but the discrepancy remained reasonable. The variations of resistances and capacitances with respect to inhibitor concentration determined by regression calculation are presented in Fig. 7.

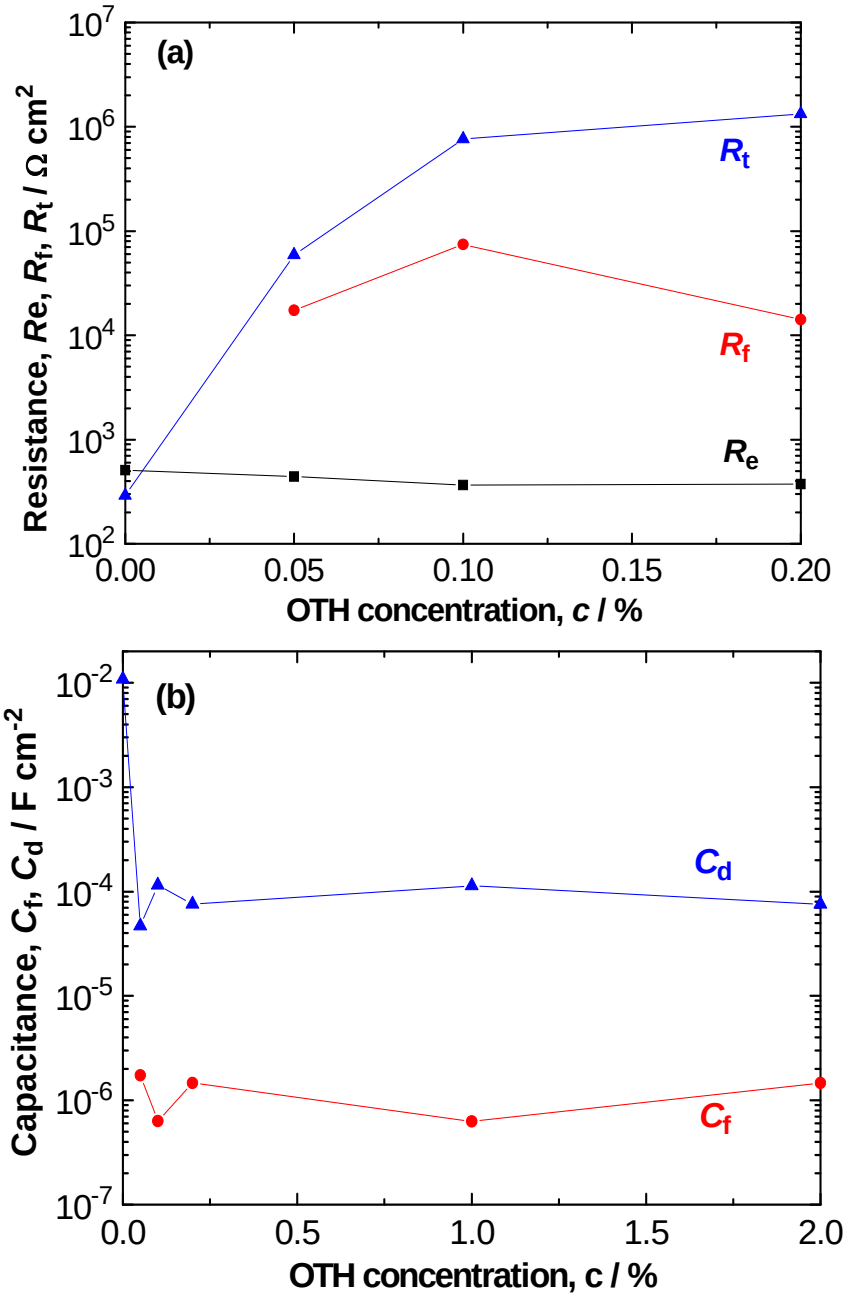

Fig. 7. Variation of resistances and capacitances determined by regression calculation on the results presented in Fig. 5 with the equivalent circuit of Fig. 6

The electrolyte resistance R_e is close to 500 Ωcm^2 in agreement with the electrolyte resistivity of the test solution. In presence of OTH, this resistance decreased. A good fitted data with only one capacitive loop for the impedance spectrum obtained in absence of inhibitor suggests that the electrode behaviour can be presented by the charge transfer resistance in parallel with the double layer capacitance [20]. It can be noticed also that in presence of OTH, the high frequency capacitive loop allocated to the surface film formed by the corrosion inhibitor on metallic surface is in agreement with previous papers [21].

The film resistance was about several tens' kΩ cm^2 and does not change at higher OTH concentration (up to 0.2%). The surface film formed by OTH addition is well impermeable towards ionic conduction. The film capacitance C_f also changes little with OTH concentration increase, and which value is about 1 μF cm^{-2}. If a planar condenser model is applied, the thickness of this film is between 300 nm to 1 μm according to the relative dielectric constant used: 3 for organic layer and 10 for the mixture of OTH inhibitor and iron oxide.

The charge transfer resistance, 290 Ω cm^2 in absence of inhibitor, increased significantly by addition of OTH, and reached 1.3 MΩ cm^2. A further addition of OTH however does not lead to an increase *of* R_t.

The value of C_d, double layer capacitance is very high, ca. 10 mF cm^{-2}. Such a high interface capacitance is sometimes encountered for the corrosion of steel, and corresponds likely to the accumulation of corrosion products, such as C and Mn which do not dissolve in the corrosion test solution. These elements remain therefore at the electrode surface, and since they are electronic conducting species, the electrode/electrolyte interface area becomes huge. In presence of inhibitor, the value of the capacitance 100 μF cm^{-2} is closer to the double layer capacitance often reported in the literature. Note, however, that this value is too high for a dilute solution, and thus a similar roughening or accumulation of corrosion products at the electrode surface may happen, but much reduced extent.

The corrosion inhibitive efficiency may be calculated from the impedance data. Stern and Geary showed the relationship between the polarization resistance R_p and the corrosion current density I_{corr} [19]. In the particular case examined in this paper, the R_t is more closely correlated with the corrosion rate [22].

$$I_{corr} = \frac{B}{R_t} = \frac{1}{R_t} \cdot \frac{1}{b_a - b_c} \tag{5}$$

This equation is derived directly from Eq. (2). To evaluate the corrosion current density, therefore, the Tafel constants b_a and b_c should be evaluated. For this sake, these values were extracted from the polarization curves presented above (Tables 3 and 4): b_a from the anodic scan and b_c from cathodic one. Fig. 8. presents the variation of b_a, b_c, and (b_a,-b_c) with respect to the OTH concentration.

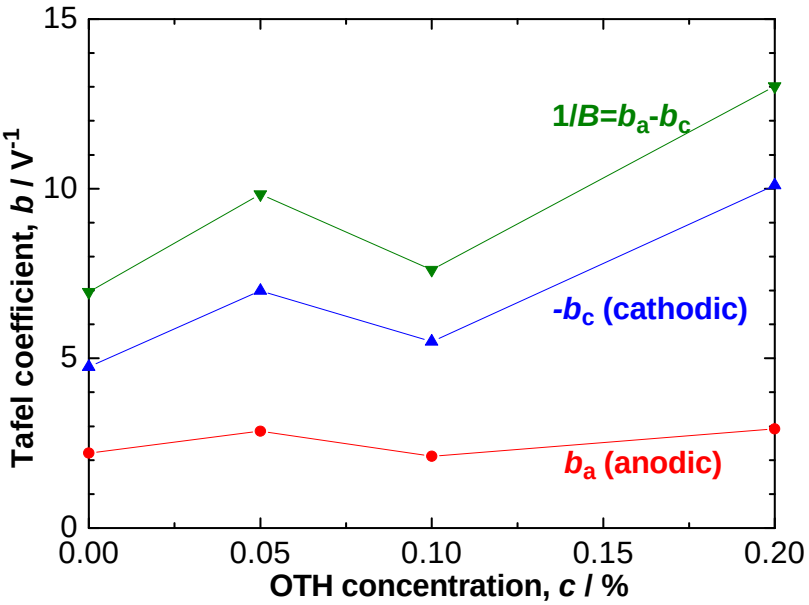

Fig. 8. Dependence of Tafel constants with respect of OTH concentration determined from cathodic ($-b_c$) and anodic (b_a) potential scan

It can be seen that b_a value remains small, less than 3 V^{-1}, and does not depends on OTH concentration in agreement with the passive state of carbon steel electrode. The cathodic Tafel constant, b_c in absolute value, increases slightly with OTH concentration. As the whole, 1/B value increases, from 7 V^{-1} in absence of inhibitor to 13 V^{-1} at the OTH concentration equal to 0.2% (Table 7).

Table 7. Corrosion current density and inhibitive efficiency evaluated from the electrode impedance. Carbon steel in the corrosion test solution. Disk rotation speed=600 rpm

OTH (%)	*1/B* (V^{-1})	I_{corr} (µA cm^{-2})	I.E. (%)
0	7	494	--
0.05	9.8	1.73	99.65
0.1	7.6	0.172	99.97
0.2	13	0.0579	99.99

It can be seen that in absence of inhibitor, the corrosion current density is slightly greater than that determined from anodic polarization (Table 6; 294 µA cm^{-2}) but remains in the same order of magnitude. In contrast, the corrosion current density is significantly smaller for OTH concentration greater than 0.1%. The inhibitive efficiency is greater than 99% indicating highly protective effect of OTH for carbon steel.

3.4.2. Influence of immersion time

Fig. 9 presents the effect of the immersion time on the impedance spectra at the corrosion potential; the inhibitor concentration was set at 0.2%.

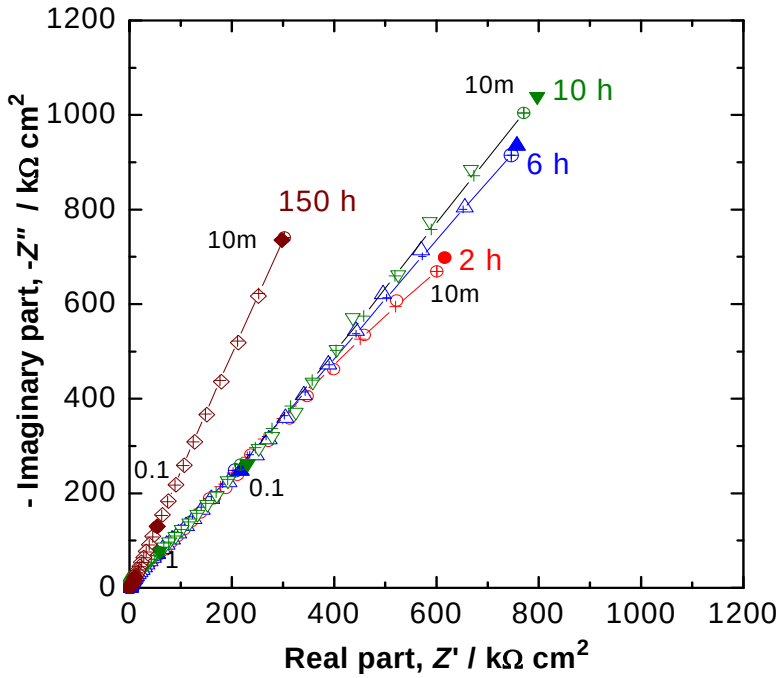

Fig. 9. Impedance diagrams of carbon steel in IRW+0.2% OTH for different immersion times; Disk rotation speed=600 rpm

The impedance diagram in Nyquist plot showed a straight line of the slope close to one for a short immersion time, and then it remains straight line but becomes steeper. To represent this straight line, a blocking CPE was added to the equivalent circuit presented in Fig. 6 as sketched in Fig. 10.

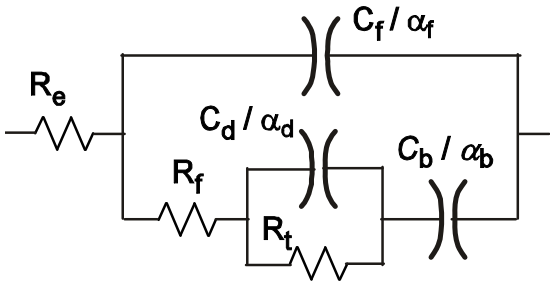

Fig. 10. Electrical equivalent circuit used to reproduce the impedance spectra presented in Fig. 9

As can be seen in Fig. 9, the comparison of experimental impedance spectra and calculated one by Simplex regression showed a good agreement between them attesting the validity of equivalent circuit adopted. The variation of different elements in Fig. 9 used for regression by Simplex method is presented in Fig. 11. In contrast, the charge transfer resistance R_t continue to augment and stabilize after four days. The effect of OTH is thus double; in the first it enhances the barrier property of the surface film, but its effect is limited in the time; in the second it inhibitive effect improves with immersion time. The corrosion current density becomes therefore significantly smaller than that evaluated in two-hour of immersion time. The thickness loss of carbon steel becomes close to 10 nm y^{-1}, if these experiments are valid, in spite of a marked extrapolation of impedance spectra to evaluate them.

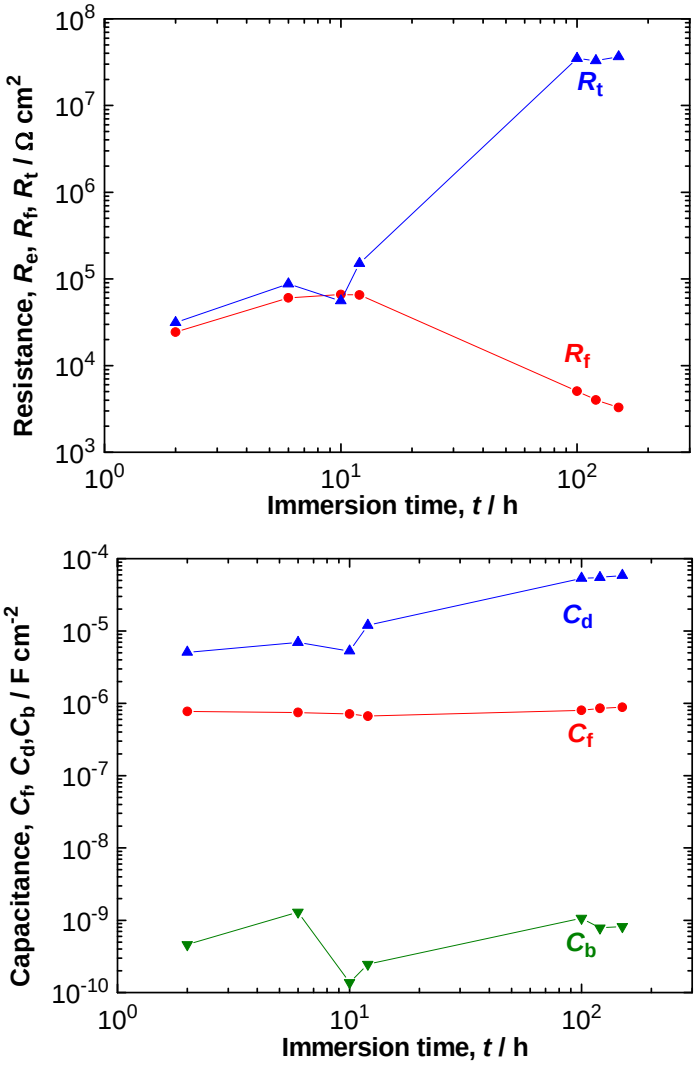

Fig. 11. Variation of circuit element values with immersion time for the impedance spectra presented in Fig. 9

The film capacitance C_f remains essentially constant, that is the film thickness itself seems not to change with time. The variation of R_f is thus more closely related to its permeability towards ions. C_d increases in the factor of ten within six days, the electrode becomes rougher by corrosion process. The accumulation of corrosion products in the surface film may also explain these two variations. C_b values remains almost constant all through the experimental period, and values ca. 0.5 nF cm^{-2}. The CPE coefficient remains close to 0.5 even when the capacitive branch becomes markedly steeper than the unit slope; therefore, the blocking capacitance introduced in the reaction model is likely due to the diffusion process. The Warburg impedance Z_W is expressed as:

$$Z_W = \frac{\sigma}{\sqrt{j \cdot \omega}} = \frac{1}{\sqrt{j \cdot C_b \cdot \omega}} \approx \frac{45000}{\sqrt{j \cdot \omega}} \quad (6)$$

If the diffusion coefficient D is estimated as 10^{-5} cm^2 s^{-1}, usual value in aqueous medium, then the concentration of diffusing species can be estimated as 7×10^{-6} $molcm^{-3}$. Though this species is unknown, the value of concentration corresponds to weakly dissolving compounds.

4. CONCLUSION

In this study we have shown the good inhibiting effect of OTH formulation containing *Opuntia ficus indica* seed oil, against carbon steel corrosion in an acid medium. OTH causes a decrease of both anodic and cathodic current density values. The inhibitor studied acts by modifying the kinetic of processes taking place at the carbon steel/ acid medium interface. The OTH may be considered a mixed corrosion inhibitor; it appears therefore as a promising protection system for carbon steel, both by its efficiency and by an “environmentally friendly” property. The protective effect of OTH when added at the concentration of 0.2% hinders the propagation of pitting corrosion, and the inhibiting efficiency improves with immersion time. The corrosion rate estimated from the EIS data indicates that the corrosion protection of carbon steel by OTH is largely "assured".

Acknowledgements

This work was in part financially supported by the PROMET project and we would like to acknowledge the LISE laboratory (Paris VI-France) for its collaboration through CNRS-CNRST project under PICS n°3388.

REFERENCES

[1] C. Yalçin, and A. Tekin, J. Sci. Food Agr. 83 (2003) 846.

[2] M. Ennouri, E. Bourret, L. Mondolot, and H. Attia. Food. Chem. 93 (2005) 431.

[3] B. Matthaus, and M. M. Özcan. Sci. Hortic. 131 (2011) 95.

[4] N. Chougui, A. Tamendjari, W. Hamidj, S. Hallal, A. Barras, T. Richard, and R. Larbat, Food Chem. 139 (2013) 796.

[5] Ranscher, G. Kutsan, R. Bandula and T. Szailer. Proceedings of the 9th European Symposium on Corrosion Inhibitors,Ann. Univ.Ferrara, N.S, Sez. V, Suppl. N. 11 (2000) 105.

[6] A. Y. El-Etre, M. Abdallah, and E. El-Tantawy, Corros. Sci. 47 (2005) 385.

[7] A. Y. El-Etre, Corros. Sci. 45 (2003) 2485.

[8] A. Ostovari, S. M. Hoseinieh, M. Peikari, M. S. R. Shadizadeh, and S. J. Hashemi, Corros. Sci. 51 (2009) 1935.

[9] K. O. Abiola, and J. O. E. Otaigbe, Corros. Sci. 51 (2009) 2790.

[10] J. C. Da Rocha, J. A. D. C. Ponciano Gomes, and E. D'Elia, Corros. Sci. 52 (2010) 2341.

[11] N. Hajjaji, N. Bettach, H. Hammouch, A. Srhiri, A. Dermaj, and D. Chebabe. OMPIC Morocco Patent N°3069/10 (2011).

[12] M. Boujnah, *Dossier* du Colloque de la 2éme Journée de la Culture du Cactus d'El kalâa. Morocco (2000).

[13] F. Salvo, E. MGalati, S. Locurto, and M. M Tripodo, IV International Congress on Cactus Pear and Cochineal (2002).

[14] N. Tlili, N. A. Bargougui, W. Elfalleh, S. Triki, and N. Nasri, J. Med. Plants. Res. 5 (2011) 4519.

[15] W. M. Breene, S. Lin, L. Hardman, and J. Orf, J. Am. Oil. Chem. Soc. 65 (2007) 1927.

[16] I. El Mannoubi, S. Barrek, T. Skanji, H. Casabianca, and H. Zarrouk. Chem. Nat. Comp. 45 (2009) 616.

[17] M. M. Özcan, and F. Y. Al Juhaimi, J. Food. Sci. Nutr. 62 (2011) 533.

[18] P. Keller, Werkst. Korros. 20 (1969) 102.

[19] M. Stern, and A. L. Geary, J. Electrochem. Soc. 104 (1957) 56.

[20] P. Bommersbach, C. Alemany-Dumont, J. P. Millet, and B. Normand, Electrochim. Acta 51 (2005) 1076.

[21] A. Srhiri, Y. Derbali, and T. Picaud, Corros. Sci. 50 (1995) 788.

[22] I. Epelboin, M. Keddam, and H. Takenouti, J. Appl. Electrochem. 2 (1972) 71.